Copyright 1999, Society of Photo-Optical Instrumentation Engineers
This paper was published in Optical Microlithography XII, Volume 3679 and is made available as an electronic reprint with permission of SPIE. One print or electronic copy may be made for personal use only. Systematic or multiple reproduction, distribution to multiple locations via electronic or other means, duplication of any material in this paper for a fee or for commercial purposes, or modification of the content of the paper are prohibited.

Imaging contrast improvement for 160nm line features using sub resolution assist features with binary, 6% ternary attenuated phase shift mask with process tuned resist

Nishrin Kachwala(1), John S. Petersen(2), J. Fung Chen(3), Mike Canjemi(4), Martin McCallum

1. SEMATECH , 2706 Montopolis Drive, Austin, TX 78741-6499
   Nishrin.Kachwala@sematech.org
2. Petersen Advanced Lithography, PO Box 162712, Austin, TX 78716
3. Microunity Systems Engineering Inc., 475 Potrero Ave., Sunnyvale, CA 94086-4118
4. Microelectronic Engineering Dept., Rochester Institute of Technology, 82 Lomb Memorial Dr., Rochester, N.Y. 14623-5604
5. INTERNATIONAL SEMATECH , 2706 Montopolis Drive, Austin, TX 78741-6499

ABSTRACT

The process window for a particular feature type can be improved by improving the aerial image or tuning the resist process. The aerial image can be improved by means of illumination or by means of mask enhancements. The illumination can be on-axis or off-axis tuned to feature type and mask. Mask enhancements being OPC and phase shifting. We illustrate process window improvement by imaging enhancement with binary and attenuated mask, with conventional and annular off-axis illumination, with and without OPC. The OPC is Sub resolution assist features (SRF). The SRF structure modifies the aerial image of the primary feature and allows for reducing dense-iso bias across pitch leading to a larger overlapping DOF across multiple pitches (ODOF). Across pitch studies with a binary mask were carried out for semi-dense and isolated lines. This study was conducted with two types of resist. A low contrast resist process tuned for isolated lines patterned on an ASML/300 stepper (0.57NA with 0.6/0.8 annular and 0.75 sigma conventional illumination). And a high contrast resist tuned for dense lines patterned on a SVGL Micrascan 3 (0.6 NA with 0.8σ conventional, and 0.6/0.8 annular). Reported results are process improvements across pitch, developing process with scattering bars and not printing of side lobes.

Simulation results with low and high contrast resist, Binary vs. 6% transmission masks will also be reported. PROLITH/3 simulation study conducted with a low contrast resist suggested that the isolated line resist would print the 80nm sub resolution features at sizing. Further, that a high contrast resist would not print them at sizing but would print them when the 160nm lines were sized roughly 10% larger (under exposed) region. Thus far, at sizing, the experimental results matched prediction; the low contrast resist process printed the sub resolution features. As for process window matching across the chosen pitches, this process showed an imperfect solution with over exposure to eliminate the sub resolution patterns. Simulations appear to make good predictions for the two cases (high vs. low contrast resist with binary mask) examined and make it possible to explore better solutions. For instance, under a fixed set of develop and PEB conditions, analysis of infinite contrast resists did not move the danger of sub resolution features printing much above the +10% CD sizing. However using a 6% ternary attPSM moved the printing limit to +20% of target CD size. The results of process window improvements with an attenuated PSM (6%) using a high contrast resist will be discussed. In all the cases, sub resolution feature OPC for isolated lines was compared with no OPC feature.

Keywords: Ternary Attenuated PSM, OPC, and scattering bars, side lobes

INTRODUCTION

Optical lithography was predicted to run out of steam a couple of decades ago. Today optical lithography at 248 nm is being used at 180nm node. 193nm lithography was predicted to be used at the 150-nm node per the SIA roadmap. But, due to lack of production level tools at 193nm, optics lifetime issues, resist maturity at 193nm (due to lack of etch resistance comparable to 248nm DNQ resists, Line edge roughness, mechanical stability and outgassing of resists) lithographers are pushing 248nm as far as the 130nm node with resolution enhancement techniques.

Our approach to extending working at optical wavelength has been one of imaging process integration. By imaging process we treat the mask, the imaging system and the resist as a complete integrated system. In this study we will talk about

248nm optical extension, but the principles could be applied to any optical wavelength. To extend the 248 nm wavelength we use a variety of masks, which includes strong and attenuated PSM, that have OPC. The imaging system being conventional or off-axis illumination, including aberrations in the lens. Taking into account aberrations in the imaging system becomes important as we push geometries much below the imaging wavelength. Integrating resist with mask type and illumination condition is another important aspect of optical extension(1). Resist are tuned for feature types, dense or isolated as well as mask type for e.g.: resist with high surface inhibition are required for not printing side lobes with attenuated contact hole masks. One must manage the complexity of the imaging integration process and make it cost effective.

MANIPULATION OF IMAGING CONTRAST TO IMPROVE PROCESS WINDOWS

In lithography, a critical parameter is the resist line width. A metric that affects the edge definition of the resist pattern is the slope of the aerial image intensity relative to the horizontal position. Through the measurement of the Normalized image log slope (NILS) one can judge the performance of resist images at different $I_{thresholds}$. Other factors that affect the resist edge definition are its composition, absorbency, the post exposure bake, the developer composition, develop conditions, substrate reflections and compatibility. The transfer of the aerial image into the resist forms a gradient of dissolution rates which gives rise to the final resist image after PEB and development. The final resist profile is a function of the resist contrast and the optical contrast. We call the imaging contrast (ImgC) a combination of the resist contrast and the aerial image contrast. By increasing the optical contrast of the image or using a higher contrast resist under a fixed set of develop and PEB conditions the ImgC can be improved. For positive DUV resist, the resist contrast can be adjusted within limits with PEB and develop conditions. The aerial image contrast can be varied by NA, λ, the illumination conditions or mask.

From Figure 1 we see that Alternating PSM will give us the best aerial image contrast improvement for a properly chosen value of partial coherence (between 0.3-0.4). The next choice would be a 6% attenuated mask using partial coherence between 0.55-0.8. Alternating PSM was not explored in this study. We chose a 6% attenuated PSM for improving the aerial image.

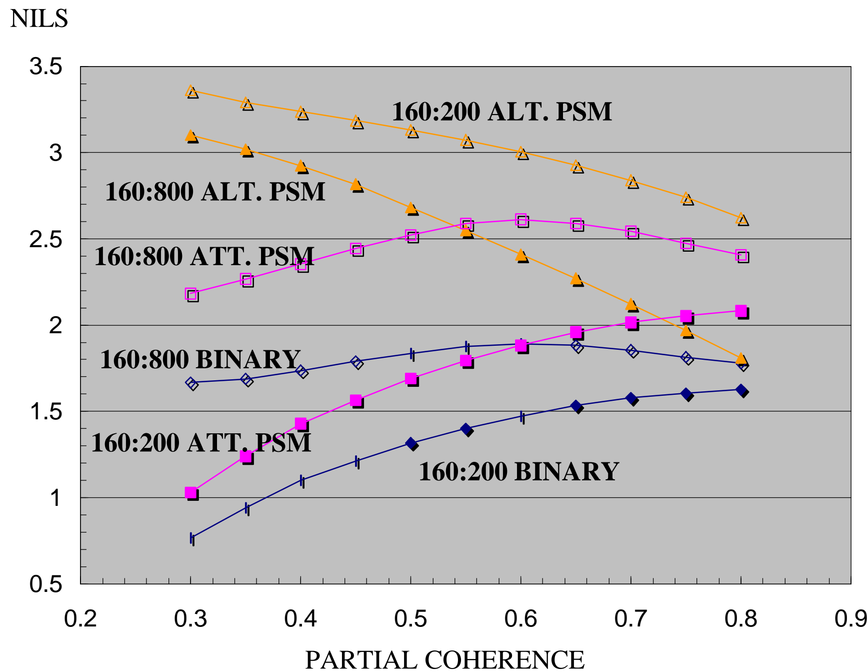

Figure 1 NILS versus partial coherence for various mask enhancements for dense and isolated features for a 248nm exposure with 0.6NA

For illumination we chose two conditions, conventional with partial coherence of 0.8 and annular with 0.6 inner σ and 0.8 outer σ. Simulations showed that more coherent setting (smaller σ) does not work well for AttPSM line features through defocus. The annulus was optimized for the 1:2 feature.
Since AttPSM is a weak phase-shifter, it permits zero order diffraction to enter lens pupil. Hence, the NA and partial coherence were optimized in the same way as typically done for binary chrome mask.

BINARY MASK WITH A LOW CONTRAST RESIST

The goal of this work is to image 160 nm features with 1:2 pitch and isolated feature for gate level applications with a reasonable process window, keeping the options for mask, resist and imaging as simple as possible. The success criteria being 0.6µm overlapping depth of focus (ODOF) at 6% Exposure latitude (EL).

We chose to start with a simple binary mask, with conventional illumination and low contrast resist UV5 from Shipley. Why low contrast resist? For k_1 <0.5, small dense features have their conjugate point at the half pitch(10). This conjugate point moves away from the target size as we go to larger pitches. Inducing an imaging bias with resist to bring the conjugate point closer to the target size for pitches >1, for optimum imaging. We picked low contrast resist since they provide a large resist bias(3).

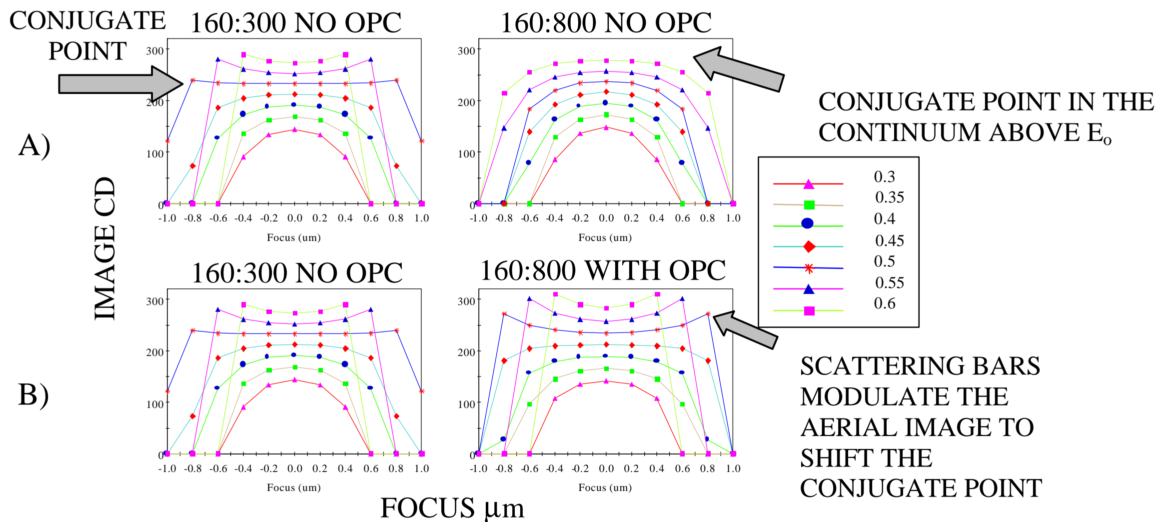

Figure 2: Image CD versus Focus for the dense (1:2) feature and isolated feature (1:5) A) without OPC on the isolated feature B) With SRF OPC on the isolated feature with 0.57NA and 0.63σ, 248nm exposure

Process conditions: A 0.57 NA, 0.63 σ ASML/200 248nm DUV stepper was used. Resist thickness was 536 nm with 57 nm of DUV32 BARC.

With conventional Illumination a depth of focus (DOF) of 0.55µm for the 1:2 pitch and 0.65µm for the isolated at 6% EL was obtained. There was no ODOF at 6% EL between the two features. Thus these conditions did not meet our ODOF success criteria. To improve the DOF on the dense features annular off axis illumination was considered. This is an example of image contrast enhancement. Annular illumination was chosen with a 0.6 inner σ and 0.8 outer σ on an ASML/300 stepper. Annular illumination gave us 0.8µm DOF for the 1:2 and 0.50µm DOF for the isolated at 6% EL. There was no ODOF at 6% EL. It is well known that OAI will affect Optical proximity effects (5). Thus to enhance the DOF of dense features with OAI and keep the performance of the isolated features one can apply scattering bar OPC to the isolated features. To keep the OPC simple scattering bars were applied to isolated features only.

What do the scattering bars do? In Figure 2, Image CD versus focus for dense (160:300) and isolated line is shown. The conjugate point for the dense line is around 230 nm, which is as predicted, at the half pitch for dense features for k1 <0.5. The conjugate point for the isolated features is in the continuum near the maximum of the aerial image. In order to have better match of performance between the pitches we need to bring the conjugate point for the isolated feature closer to the

target size. That is making the isolated features appear “dense-like”. By adding sub resolution assist features (SRF) close to the main feature (Figure 3), the conjugate point can be moved from the continuum closer to the target feature size. The SRF modulate the Aerial Image width and the log-slope of the feature to create an isofocal region.
Fung et al (4) predict the features to be of the order of (λ/5) – (λ/3) and its optimum separation of the scatter bar from the main feature edge to be of the order of λ. This rule allows the sidelobe intensity to be less than 0.4 to avoid imaging the SRF, assuming the printing threshold to be around 0.3 to 0.4.

With OPC on the isolated feature, the best overlap was achieved with an 80-nm scattering bar distance 240 nm from the main feature edge. The ODOF was 0.6 µm at 6% EL. However, as shown in Figure 4 the scattering bars were imaging at the same exposure that was sizing at 160nm lines which was 1.7 times the Dose to clear (Eo). We found that overexposing the features eliminated the printing of the sub assist features. Thus applying a bias to the features would help eliminate this problem. Another option would be to improve the “imaging contrast” to get rid of the sidelobes.

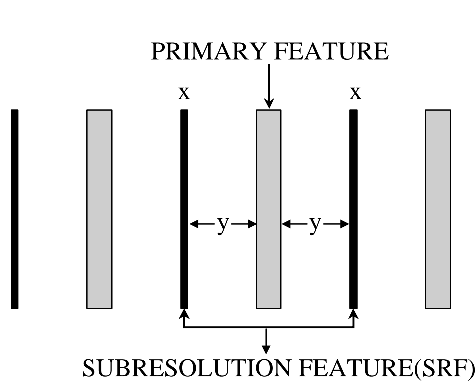

Figure 3: Schematic showing the subresolution feature of size x nm

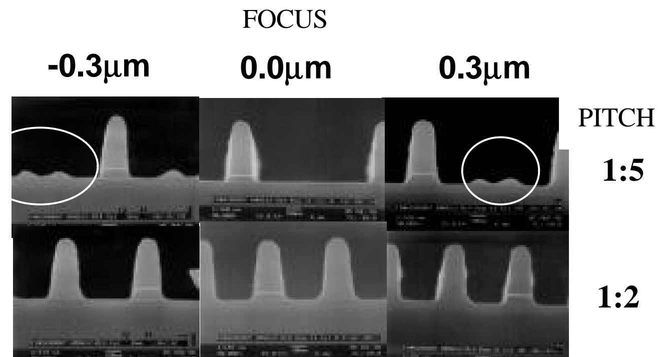

Figure 4: SRF imaging at dose to size with the low contrast resist

As seen in Figure 4, for the low contrast resist the “imaging bias” was such that the sidelobes of the subresolution features (SRF) were sampled (n=4). By increasing the contrast of the resist (n=10) this can be avoided (Figure 5). The “imaging bias” which is a convolution of the aerial image NILS of the sampled image CD and the resist bias. A resist with an imaging bias such that it samples the aerial image below the intensity level of the sidelobes, thus not imaging the sidelobes of the SRF(Figure 6a). The resist bias depends on the polymer chemistry, acid diffusion, development rate, absorption, reflection and PEB conditions. Whereas the bias contribution from the aerial image bias depends on illumination condition, mask type, feature pitch and duty cycle. Interaction of the resist with the aerial image, its subsequent bake and development which finally results in the resist CD arises from the total imaging bias. Because the resist bias is convoluted with the NILS it is difficult to measure its bias. We have proposed a way in which it can be estimated if the isofocal region is known. To interpret the data we made an estimate of where the aerial image was sampled by determining the imaging bias using the technique described in the next section. We varied the contrast of the resist till we found an n-value that gave us the correct bias. In this way we were able to reproduce the imaging of the scattering bars and explore process design fixes that led to higher n (resist contrast).

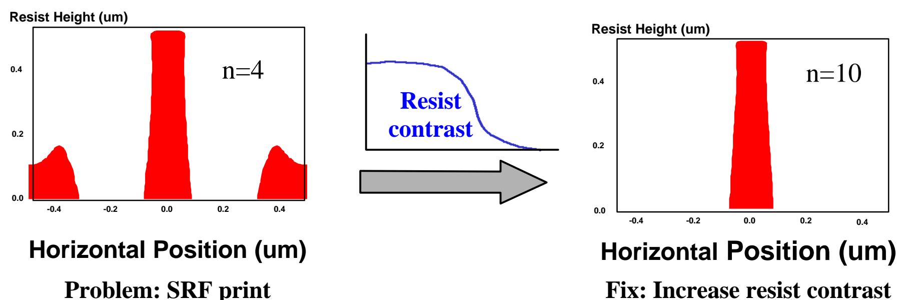

Figure 5: Varying resist contrast to prevent the SRF from imaging

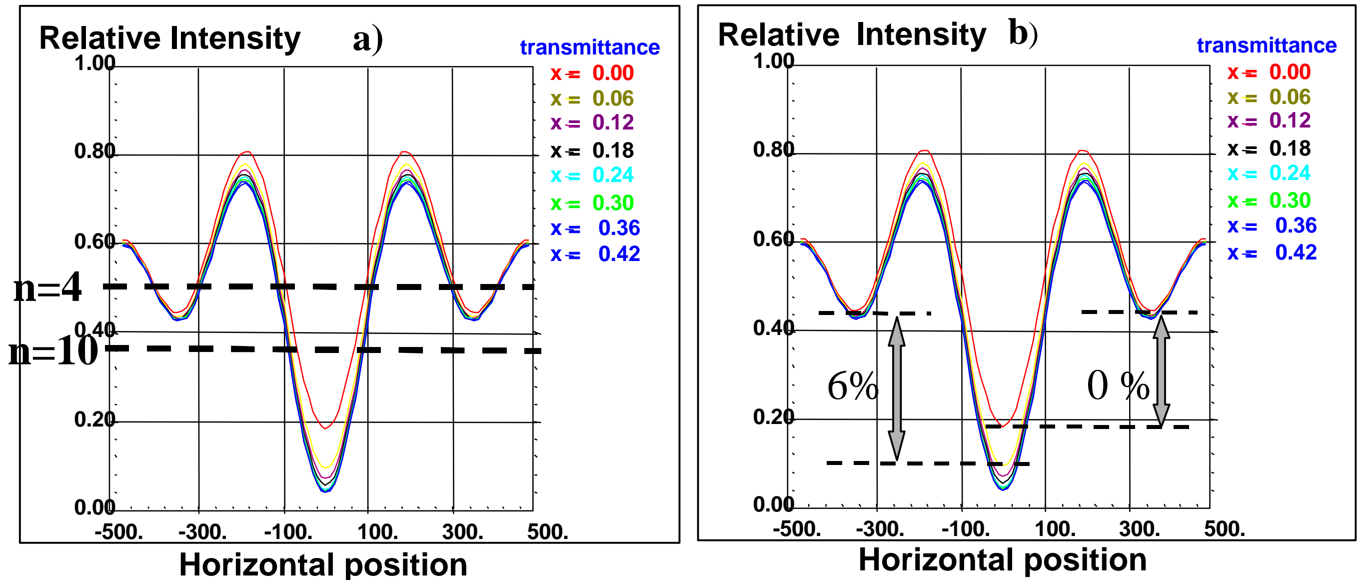

Figure 6: a) Different resist contrast sample different thresholds on the aerial image b) Image contrast increases with % Transmission

The imaging bias evaluation of 6% attenuated mask.

To properly tune an imaging bias it is important to know the NILS and Image CD that is sampled on the aerial image. The image CD dependence on focus for different intensity threshold is generated from PROLITH/2 for 400-nm pitch. The intensity was translated to dose relative to the experimental isofocal region dose using Equation 1. The advantage lies in the fact more data from a focus exposure experiment can be utilized, plus aberrations can be added if needed to make the final bias assessment.

$$Dose \cong [1/Intensity] \cdot Intensity_{IFR} \cdot Dose_{IFR}^{EXPERIMENTAL}$$

Equation 1: Aerial image intensity translated to dose relative to the experimental Iso-focal region (IFR) Dose

From PRODATA the experimental and threshold resist process windows were calculated. The threshold resist process window was given a focus offset of 0.2µm to match the experimental window in focus, then the data was given an image bias offset to get dose match. A bias of 65 nm matched the process windows as shown below in Figure 7. The slight mismatch, since we haven't accounted for aberrations and effects of focusing into the resist versus outside of it have on the formation of the latent image. Then knowing bias we determined the n value needed to replicate the bias in our lithography simulator.

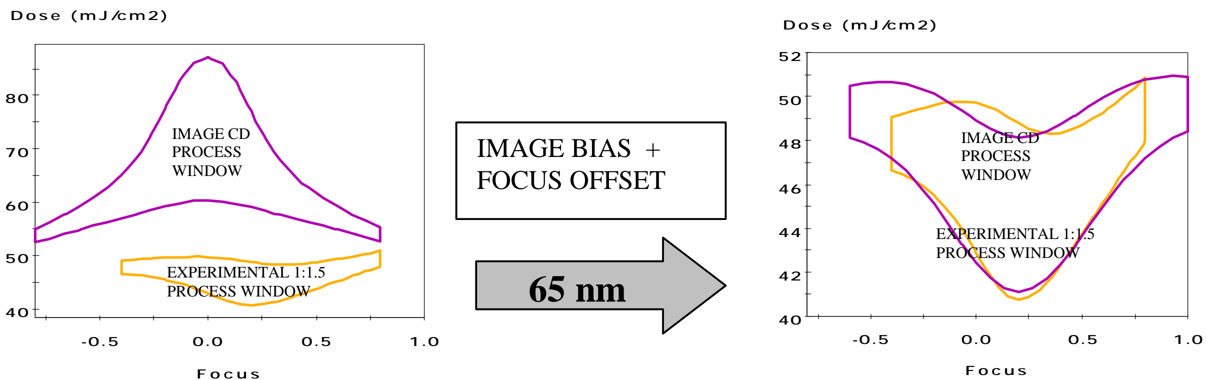

Figure 7: Matching of Image CD and experimental process windows to estimate the image bias for 6% attenuated phase shift mask

CHANGING RESIST CONTRAST TO ENHANCE PROCESS WINDOW

After PROLITH/3D was calibrated for a proper imaging bias as discussed in the previous section, simulations were done varying the contrast of the resist for the 160nm isolated feature with a 80nm SRF distant 240nm from the main feature edge. A contrast between 6 and 10 eliminated the SRF from printing. Since a high contrast resist has a nonlinear response (3) to exposure sidelobes are less likely to print.

For improving the ImgC with a resist, we chose a fairly high contrast resist (n=12) from JSR M20G (420nm) and DUV30 BARC (60nm) from Brewer Science. Any imaging results reported from now on was with the high contrast resist, with an SVGL MS3 248nm DUV step and scan system with a 0.6NA. Conventional illumination with 0.8σ and off-axis with a 0.6/0.8 annulus was used. We use the same success criteria as before i.e. an ODOF of 0.6μm at 6% EL. For the low contrast resist the SRF were printing at dose to size which was $1.7E_o$, with the high contrast resist the SRF were printing at $1.6E_o$, whereas the dose to size was at $2.1E_o$. Thus using a high contrast resist pushed the imaging of the SRF to just outside the ±10% CD limits. There was some ODOF but none at 6%EL between the pitches 1:2 (460nm) and 1:5(960nm) (Figure 8). The process window for pitches 1:1.5(400nm), 1:2, 1:2.5(540nm), 1:3(620nm), 1:5, 1:30(4800nm) is shown in Figure 9. There was no ODOF between the features with conventional illumination with 0.6NAand 0.8 σ at 6% EL.

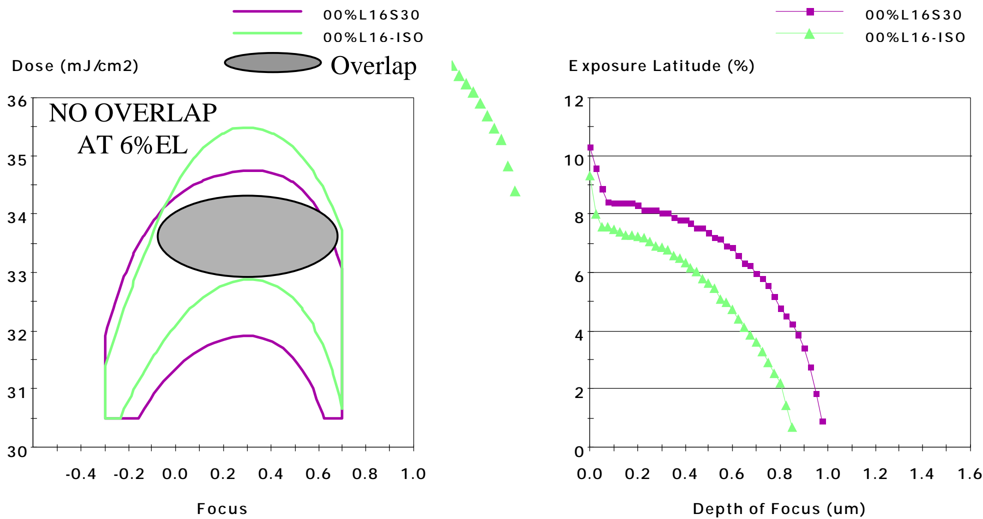

Figure 8: Binary mask with conventional illumination 0.6NA, 0.8σ and high contrast resist for 1:2 and isolated feature

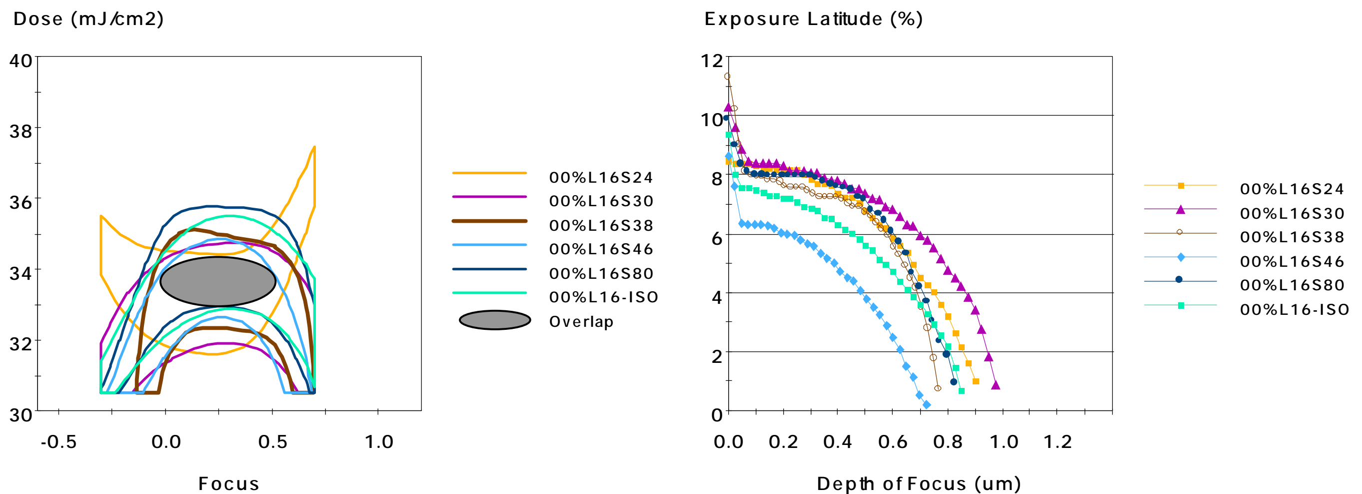

Figure 9: Binary mask with conventional illumination 0.6NA, 0.8σ and high contrast resist for pitches 1:1.5, 1:2, 1:2.5, 1:3, 1:5

With the high contrast resist we used annular illumination with 0.6/0.8 configuration to enhance the DOF on the dense 1:2 feature and overlap its process window with the isolated feature by applying OPC, same strategy as applied to the low contrast resist. There was no overlap between the 1: 2 and isolated feature at 6%EL. The EL degraded to less than 6% for almost all features as seen in Figure 10. Thus applying OPC to the isolated feature to improve the ODOF was not considered. By increasing the resist contrast we were able to avoid imaging the sidelobes, alternatively one could achieve the same effect with an attenuated PSM by improving the contrast between the SRF and the main feature as shown in Figure 5b. Increasing the NILS reduces the image bias and the resist sampling to a lower threshold on the primary image and completely to the greater than E_o continuum. The attenuated mask will also improve the overall process window.

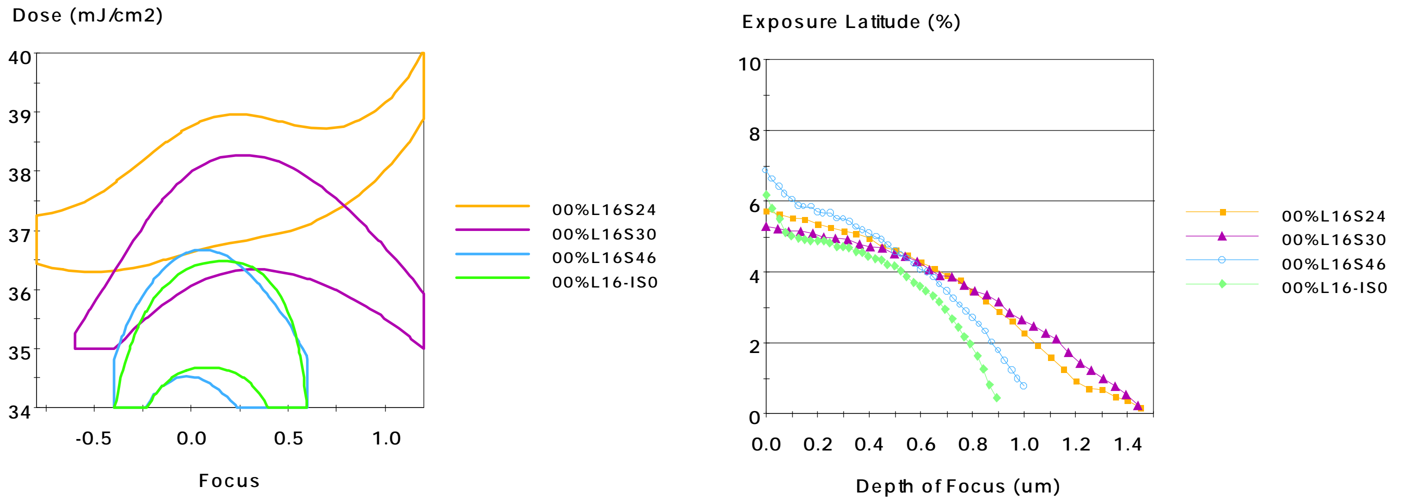

Figure 10: Binary mask with annular illumination 0.6/0.8 annulus, 0.6NA for the 1:1.5, 1:2, 1:3 and isolated features with a high contrast resist

CHANGING AERIAL IMAGE CONTRAST TO ENHANCE PROCESS WINDOW

The next step to improvement in the imaging contrast would be to use a 6% attenuated PSM, i.e. improve the image contrast. A 6% attenuated mask with Cr/CrF as the attenuated material was fabricated by DNP. The custom Line-sweeper™ mask design and OPC layout was done by Microunity. Chrome sub resolution assist bars were used as OPC features (6) and large features had Cr shields on them to eliminate sidelobe effects (7). Features larger than 300nm had chrome shields on them to suppress sidelobes and as simulation indicated prevent resist exposure through the attenuated material.

The process window curve for the attenuated mask with conventional illumination is shown in Figure 11. There was a 0.6µm ODOF at 6%EL between the dense and isolated feature. Thus using a 6% attenuated we see a reduced need for OPC between pitches with conventional illumination. Considering pitches 1:1.5, 1:2, 1:2.5, 1:3, 1:5 and isolated the ODOF at 6% EL is 0.45µm (Figure 12). The process window between the pitches requires some improvement. The isolated line, 1:2 and the 1:1.5 pitch need more overlap with the rest of the features. For the dense pitches biasing would be an option, a positive and a negative bias of 20nm was looked at, but provided an over correction. Other bias options were not available on the mask. It seems that a finer bias was required. An option would be to apply half tone biasing. Nakagawa et al (8) proposed that with half tone biasing a fine bias control could be maintained, limited by the address unit of the e-beam tool.

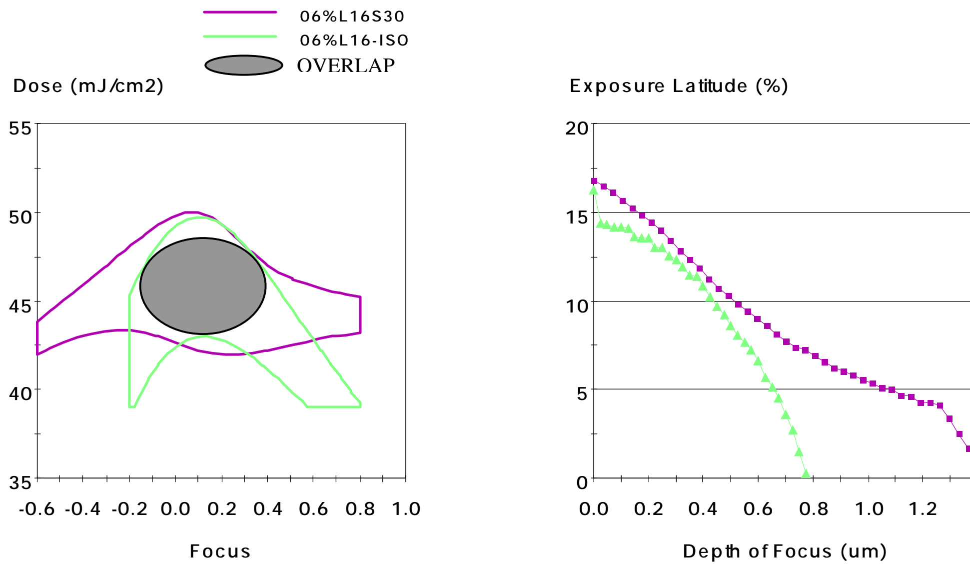

Figure 11: 6% attenuated process window for 1:2 and isolated features with high contrast resist and conventional illumination 0.6NA, 0.8σ

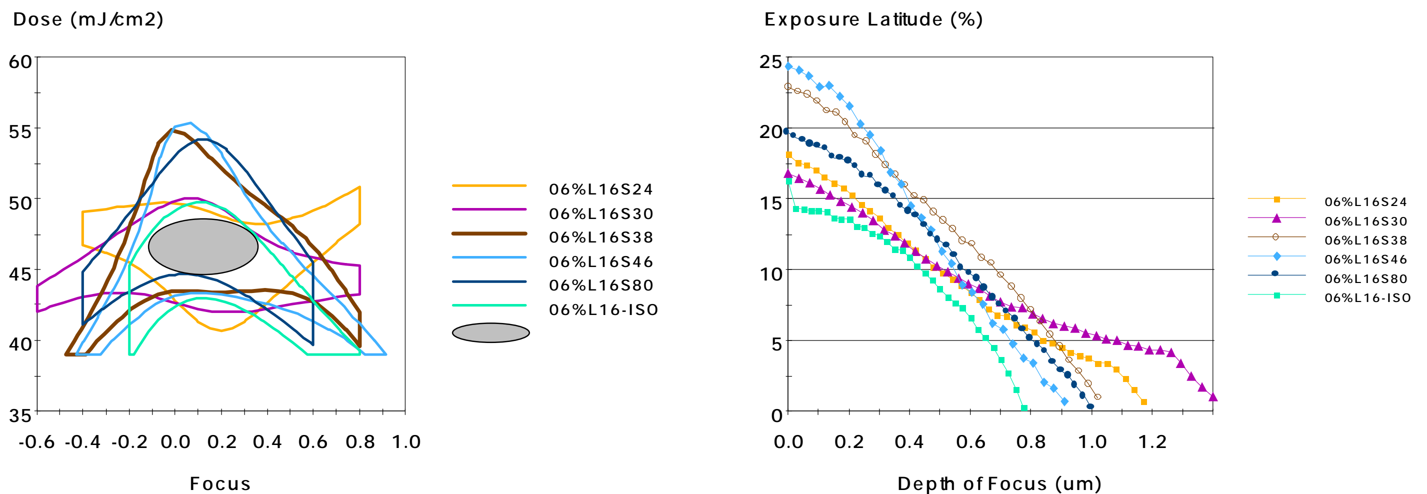

Figure 12: 6% Attenuated mask process window for 1:1.5, 1:2, 1:2.5, 1:3, 1:5 and isolated features with high contrast resist and conventional illumination 0.6NA, 0.8σ

Though we achieved our success criteria with the 6% attenuated mask and conventional illumination. To further extend the resolution to $k_1 < 0.4$ with weak phase shifting we will need off-axis illumination. The results with the 0.6/0.8 annulus are shown in Figure 13. The individual DOF improves for all pitches with OAI. There is no ODOF as expected due to enhanced proximity effect. OPC will be required on all features when considering off-axis illumination. We have shown an example (Figure 14) where by using a SRF of 80 nm distant 300nm on the isolated line allowed 0.75µm ODOF at 6%EL between 1:2 and isolated feature when there was no overlap without OPC. For isolated features one would not expect any improvement in its performance with OAI (5). Also the isolated line performance is not enhanced and will degrade, as the annular ring with is increased (9).

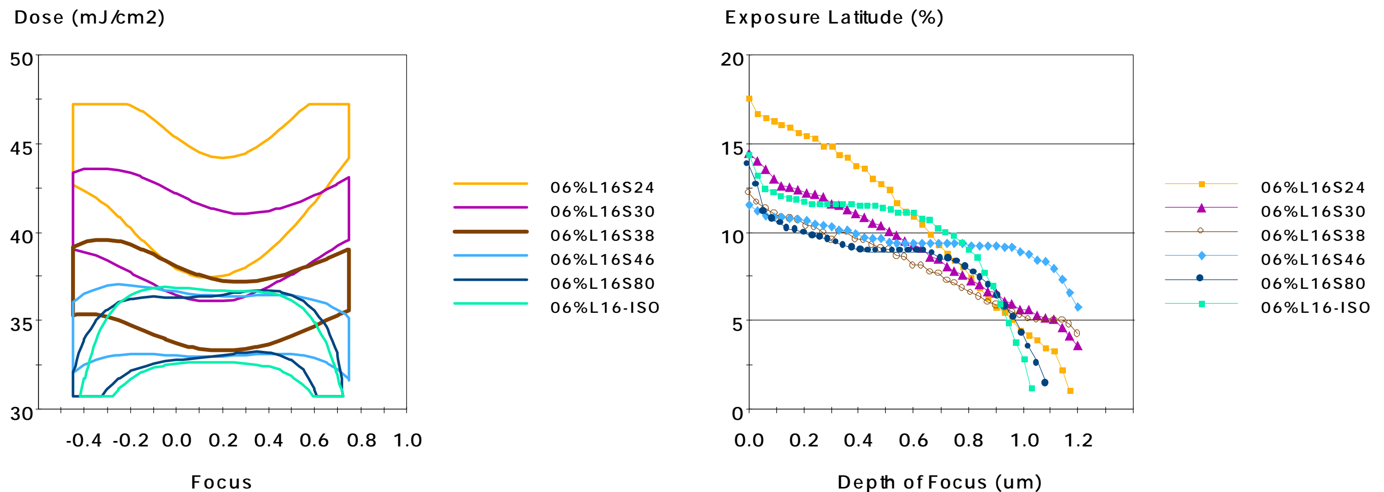

0.6NA, 6% attenuated PSM

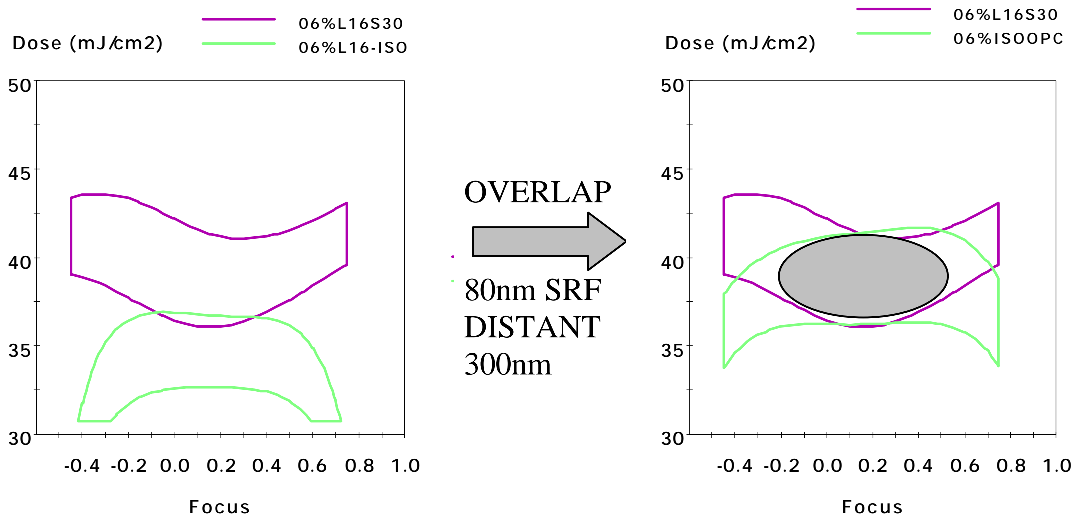

Figure 14: 1:2 and isolated feature with 0.6/0.8 annulus, 0.6NA, 6%attenuated PSM
A) No overlap without OPC B) Overlap with SRF OPC on the isolated feature

Let us try to understand the results using the normalized image log slope (NILS) as a metric for resist performance. One observes the NILS for the isolated line to degrade as we vary the inner σ of the annulus from 0.0 (conventional) to 0.8 (OAI) in Figure 15. The dense line (1:1.25) NILS improves as we go off-axis. For the 6% attenuated PSM , the NILS versus inner sigma plot shows that the 360nm and the 960nm pitch features have similar NILS when a 0.6, 0.8 annulus is used. If both features have the same image CD, then they should have overlapping FE windows, which experimentally, they do not. Examining the image CD and the NILS at the resist threshold will provide the reason for this. The resist threshold is the intensity threshold that the resist samples to make the final resist image size and, in this case, is found by adding the imaging bias of 65nm to 160nm. This places the resist threshold at an aerial image CD of 225nm for the dense lines imaged with conventional illumination. It is at this size and intensity threshold that the NILS and the focus dependence on image CD for the more isolated feature should be studied. Figure 16 shows for the 160nm line on the 360nm and 960nm pitch, (a) the aerial image using 0.8 sigma conventional illumination (0 inner sigma) and 0.6 inner and 0.8 outer sigma annular illumination; (b) the NILS dependence on horizontal position starting at the center of the line and extending to 360nm for the 160nm:200nm line:space; and (c) the same as (b) for the 160nm:800nm feature. The data pertinent to this analysis are summarized in Table 1.

In Table 1, the intensity thresholds were chosen to be 0.39 as referenced to the dense line image CD for both illuminators. Remember that the imaging bias was determined for the 160nm:200nm features using conventional illumination and that it arises from a convolution of the resist and aerial image contrast. Therefore if the NILS changes so should the bias, where the bias decreases with increasing aerial image contrast. Less bias will thus create a larger resist image even if the image CD at the resist threshold was the same for each different feature. In the case of the conventional illumination the NILS for the two pitches are disparate at the line edge, 2.35 and 2.75, but even more so at the resist threshold image CD, 1.55 and 2.2, with the 960nm pitch having the larger contrast values. Since the image CD for the dense and isolated features are similar, it is the NILS at the resist threshold that affect final sizing differences between the isolated and dense line in the case of conventional illumination. Experimentally we observe similar sizing and; as a result, while too small, there is good process window overlap for the two pitches. The fact that the NILS had little impact on sizing suggests that at this image contrast the resist is essentially a threshold detector. This means that the observed imaging bias may arise from the thermal dose received during the post-exposure-bake and to a lessor degree from develop (3). For annular illumination, there is a NILS convergence at the line edge suggesting that there should be good process window overlap for the two features. This is not observed experimentally because at the resist threshold, the image CD of the 960nm pitch structure is 45nm smaller than for the line of the smaller pitch. The NILS are 1.55 for the 360nm and 2.25 for the 960nm pitch features and as observed with conventional illumination has little impact. With this annulus, the difference for image CD requires optical proximity correction to gain useful process window overlap as shown in Figure 14.

Another point of interest is that using the annulus reduced the changes in image CD and NILS for the dense and the isolated line; thus improving the performance of both and not just the dense.

Finally, the values at the line edge do not reflect the imaging process accurately. The analysis in Table 1 shows that optical proximity correction should be done at the resist threshold image CD and, unless it is the same, not at the line edge. By using the resist threshold, the image CD for different focus conditions at that threshold and the NILS at the respective image CD more reliable optical proximity corrections by tuning the illuminator, mask type and mask design, and thus provides a more realistic correction to the imaging system.

Illumination	**Conventional 0.8 σ**		**Annulus, 0.6 inner and 0.8 outer σ**	
Feature	160nm:200nm	160nm:800nm	160nm:200nm	160nm:800nm
Bias (Figure 7)	65nm	<< 65nm	< 65nm	<<65nm
Resist Threshold Analysis (Listed as 0.0, 0.3, 0.6 μm focus setting)				
Image CD (nm)	225, 236, 316	216, 210, 140	225, 230, 240	180, 170, 124
Relative Intensity	0.39	0.39	0.39	0.39
NILS	1.55, 0.95, 0.22	2.2, 1.45, 0.72	1.55, 1.02, 0.55	2.25, 1.55, 1.02
Analysis at the160nm line edge of the 360nm pitch feature				
Relative Intensity at 160nm	0.26	0.23	0.26	0.34
Image CD at 0.26 Intensity	160nm	170nm	160nm	130nm
NILS	2.35	2.75	2.5	2.9

Table 1 Aerial image CD analysis summary from Figure 16 at 0 focus

CONCLUSIONS AND FUTURE WORK

Imaging contrast enhancements with resist and illumination can improve process windows. We see that with a low contrast resist, the total imaging bias is such that we run into the risk of printing the SRF. Biasing the mask or increasing the resist contrast, i.e. providing a smaller resist bias can eliminate this. We showed that with a high contrast resist, imaging of the SRF was pushed beyond the ±10% CD window. Binary mask with OAI gave low exposure latitude for the dense (1:2) feature. An option to improve the process window with an attenuated PSM was experimented. Attenuated PSM with conventional illumination mask showed an acceptable overlap between the 1:2 and isolated feature without any OPC. This implied less

aggressive OPC requirements for smaller features. This confirms some predictions made by Petersen et al (10). Attenuated mask with annular illumination showed a large proximity bias between pitches considered. OPC will be required with this combination of image enhancement

Summary of DOF for individual features for conventional and annular illumination with the high contrast resist is shown in Table 2 and Table 3.

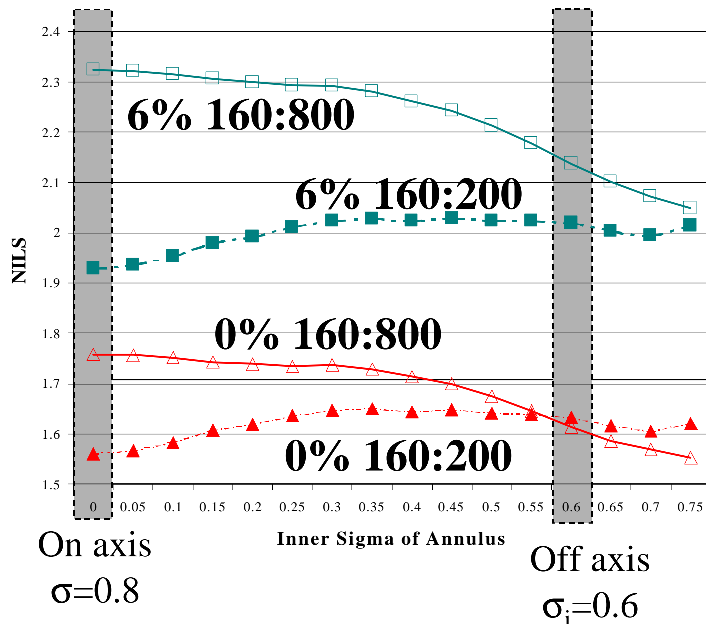

Figure 15: NILS versus Inner Sigma for binary and 6% attenuated PSM with 0.6NA

ACKNOWLEDGEMENTS

The author's would like to acknowledge SEMATECH and INTERNATIONAL SEMATECH and the Optical Extensions Technical Steering committee for their support of this project. We would also like to thank the Optical extension team member Peter Zandbergen, Manager Gilbert Shelden for their discussions and direction. In addition we would like to thank Alvina Williams and Mark Maslow for their help in this work

REFERENCES

1. B. W. Smith, L. Zavyalova, J. S. Petersen, Proc. SPIE Vol. 3334, p. 384-394 (1998).
2. J. S. Petersen, Proc. SPIE Vol. 1088, p. 540-567 (1989).
3. J. S. Petersen, J. D. Byers, Proc. SPIE Vol. 2724, p. 163-172 (1996).
4. J. Fung Chen, Tom Laidig, Kurt Wampler, Roger Caldwell, SPIE Proceedings, Vol 3051, 1997
5. W. Partlo, P. Thompkins, P. Dewa, P. Michaloski, Proc. SPIE 1927, p137-157, 1993
6. Iwasaki, Haruo; Hoshi, Keiichi; Tanabe, Hiroyoshi; Kasama, Kunihiko, Proc. SPIE Vol. 3236, p. 544-550, 1997
7. Tounai, Keiichiro; Aizaki, Naoaki, Proc. SPIE Vol. 2726, p. 82-87, 1996
8. K. H. Nakagawa, D. Van den Broeke, J. Fung Chen, Tom Laidig, K. E. Wampler, R.Caldwell, VDE Conference Proceedings of Mask Technology for Integrated Circuits and Micro-Components '98, Vol. 25, pp 139-144
9. Smith, Bruce W, Sheats, James R, Microlithography: Science and Technology, Marcel Dekker, Inc. p240-244 (1998)
10. John S. Petersen , Martin McCallum , Nishrin Kachwala , Robert J. Socha , J. Fung Chen , Tom Laidig , Bruce W. Smith, Ron Gordon , Chris A. Mack , Proc. SPIE Vol. 3546, p. 288-303 (1998).

LINE-SPACE RATIO	BINARY MASK	6% ATTENUATED PSM
1:1.25	0.33	0.55
1:1.5	0.57	0.75
1:2	0.70	0.90
1:2.5	0.57	0.85
1.3	0.56	0.67
1:5	0.60	0.72
1:30	0.43	0.60

Table 2 : Summary of DOF @ 6% Exposure Latitude for conventional illumination 0.6NA, 0.8σ

LINE-SPACE RATIO	BINARY MASK	6% ATTENUATED PSM
1:1.25	0.56	0.72
1:1.5	0.35	0.87
1:2	0.32	0.93
1:2.5	0.0	0.85
1.3	0.40	1.1
1:5	NA	0.91
1:30	0.0	0.92

Table 3 : Summary of DOF @ 6% Exposure Latitude for Annular illumination 0.6NA with 0.8σ_o and 0.6σ_i

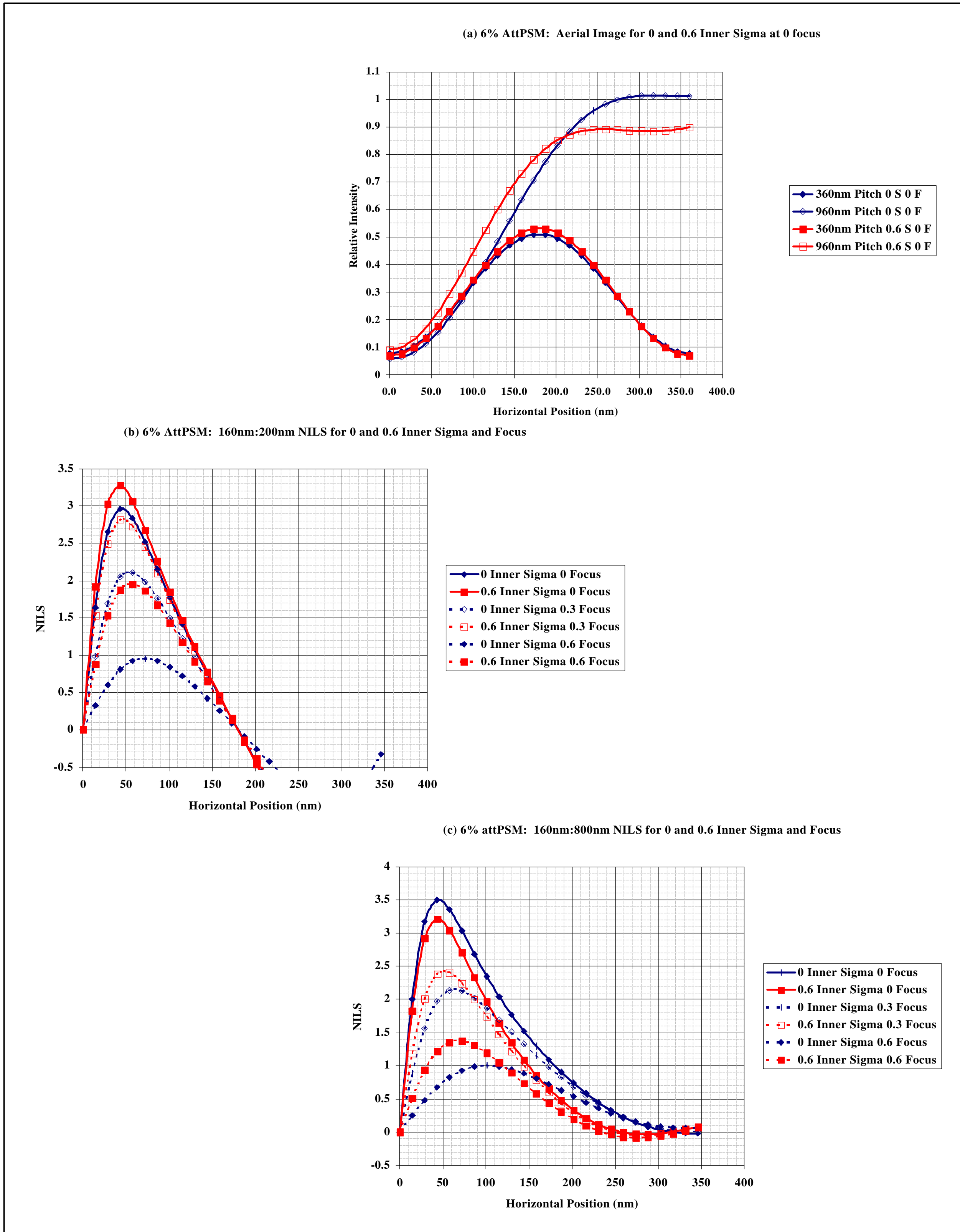

Figure 16: Image information for the 160nm line on the 360nm and 960nm pitch, (a) the aerial image using 0.8 sigma conventional illumination (0 inner sigma) and 0.6 inner and 0.8 outer sigma; (b) the NILS dependence on horizontal position starting at the center of the line and extending to 360nm for the 160nm:200nm line:space; and (c) the same as (b) for the 160nm:800nm feature.